NJC

ROYAL SOCIETY OF CHEMISTRY

COMMUNICATION

View Article Online
View Journal | View Issue

Cite this: *New J. Chem.*, 2026, **50**, 2985

Received 31st October 2025,
Accepted 19th December 2025

DOI: 10.1039/d5nj04288g

rsc.li/njc

Harnessing mitochondrial targeting: biguanide–iridium(III) complexes with enhanced anticancer activity in pancreatic cells

Sigrid Lacaille,[a] Erica Schofield,[b] Pierre Mas,[a] Robert S. Horne,[b] Barry A. Blight[b] and Andreea R. Schmitzer*[a]

Targeting mitochondrial function offers a compelling route for selective cancer therapy. We report the design, synthesis, and biological assessment of three novel biguanide–iridium(III) complexes as potent mitochondrial disruptors in pancreatic cancer cells. These complexes demonstrate markedly enhanced cytotoxicity compared to their parent biguanide ligands. Confocal imaging confirms rapid mitochondrial localization within 30 minutes, with subsequent impairment of the respiratory chain, suggesting a direct mechanism of mitochondrial dysfunction. These results highlight the therapeutic potential of iridium-based metallodrugs in targeting metabolic vulnerabilities of pancreatic cancer.

Mitochondria are central to cellular energy metabolism, producing the majority of ATP required for vital cellular functions. Beyond energy generation, they play a critical role in regulating apoptosis, making them key targets in cancer therapy. Disruption of mitochondrial function is implicated in various diseases, positioning mitochondria as attractive sites for therapeutic intervention.[1–9]

Biguanides have garnered significant interest as anticancer agents due to their protonatable nature, hydrogen-bonding capacity, and inherent chemical reactivity. Notably, metformin, originally used to treat type II diabetes, has demonstrated antiproliferative effects in pancreatic cancer cells at high concentrations, primarily through inhibition of mitochondrial complex I.[10–23] Building on this, our group reported lipophilic biguanide and biquaternary ammonium derivatives bearing alkyl and aromatic side chains, which enhanced cellular uptake and achieved low micromolar IC_{50} values, while retaining mitochondrial activity.[24,25]

Another type of chemical structure that showed interesting antiproliferative activity for the treatment of many cancers, associated with mitochondria targeting properties, is iridium(III) complexes.[26–30] In addition to being lipophilic enough to permeate cellular membranes, the photochemical properties of iridium(III) complexes allow them to be used in imaging and photodynamic therapy. Some metformin-iridium(III) complexes were previously synthesized and showed to inihibit mitochondrial respiration.[31] To date, no biguanide–iridium(III) complex has been studied for the treatment of pancreatic cancer, which accounts for one of the deadliest cancers in the contemporary world.

In this work, we designed three novel biguanide–iridium(III) complexes, **IRB1–IRB3** (Fig. 1), incorporating biguanide ligands previously shown to exhibit notable antiproliferative activity: octylbiguanide, phenformin, and phenylethynylbenzyl-biguanide. These ligands were coordinated to the dinuclear scaffold dichlorotetrakis-(2-(2-pyridyl)phenyl)diiridium(III) *via* straightforward ligand exchange reactions. The resulting complexes were fully characterized by electrospray ionization mass spectrometry (ESI-MS), as well as by ^{1}H and ^{13}C nuclear magnetic resonance (NMR) spectroscopy, confirming the successful coordination and structural integrity of the metallodrugs.

To assess the anticancer potential of the synthesized biguanide–iridium(III) complexes, their half-maximal inhibitory concentrations (IC_{50}) were determined in two pancreatic cancer cell lines: KP4 and PANC-1. To evaluate selectivity toward malignant cells, cytotoxicity was also measured in two non-cancerous cell lines: *hTERT*-HPNE pancreatic epithelial cells and IMR-90 lung fibroblasts, from which CC_{50} values were derived. The antiproliferative activity and selectivity indices of **IRB1–IRB3** were compared to their respective free ligands under identical experimental conditions (Table 1). Notably, all three complexes displayed lower IC_{50} values in cancer cells than their uncoordinated ligands, highlighting the enhanced cytotoxic efficacy conferred by iridium(III) complexation.

All three biguanide–iridium(III) complexes exhibited potent antiproliferative activity against pancreatic cancer cell lines, with IC_{50} values below 3 μM, which represents an activity 50-fold lower than that of doxorubicin for the KP4 cell line, for example.[25b] Interestingly, despite structural diversity among the biguanide ligands, the IC_{50} values of the resulting iridium complexes were

[a] *Département de chimie, Université de Montréal, 1375 av. Thérèse Lavoie-Roux, Montréal, H2V 0B3, QC, Canada. E-mail: ar.schmitzer@umontreal.ca*
[b] *Department of Chemistry, University of New Brunswick, Fredericton, NB, Canada*

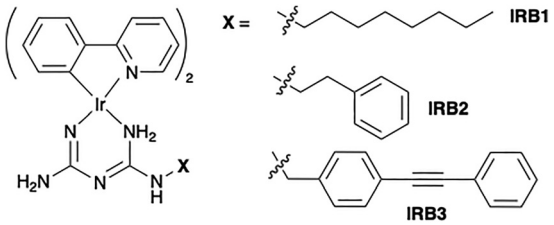

Fig. 1 Structure of biguanide–iridium(III) complexes **IRB1–IRB3**.

Table 1 IC_{50} and CC_{50} values of the biguanide–iridium(III) complexes and biguanide ligands of the cancer cell lines and healthy cell lines

	IC_{50} (μM) cancer cells		CC_{50} (μM) healthy cells	
Compound	KP4	PANC1	IMR90	*hTERT*-HPNE
IRB1	1.35 ± 0.09	2.06 ± 0.43	2.59 ± 0.25	4.20 ± 0.57
IRB2	2.40 ± 0.41	2.66 ± 0.37	3.90 ± 0.32	4.89 ± 0.73
IRB3	1.22 ± 0.12	2.18 ± 0.23	2.67 ± 0.43	3.01 ± 0.86
Octyl-biguanide	1.14 ± 0.43	6.07 ± 0.91	246 ± 57	74 ± 26
Phenformin	51[a]	180[a]	50 ± 14	335 ± 50
PEB-biguanide	6.13 ± 0.80	15[a]	22.47 ± 2.25	80.91 ± 0.44

[a] From Hébert, A. *et al*. Scientific Reports 2021, **11**(1).

remarkably similar, suggesting that coordination to iridium(III) overrides ligand-dependent variations in efficacy. For instance, while octyl-biguanide alone displayed strong activity, its coordination in **IRB1** yielded an equivalent IC_{50} in KP4 cells but significantly improved potency in PANC-1 cells, reducing the IC_{50} by threefold. Complexation of phenylethynylbenzyl-biguanide (PEB-biguanide) in **IRB3** led to five- and sevenfold reductions in IC_{50} in KP4 and PANC-1 cells, respectively. Phenformin, the least active free ligand, exhibited the most dramatic enhancement upon coordination: IC_{50} values decreased 24-fold in KP4 and 67-fold in PANC-1 following formation of **IRB2**.

This increased potency was accompanied by a concomitant rise in cytotoxicity, however, toward non-cancerous cells. Selectivity indices (SI), calculated using CC_{50}/IC_{50} ratios, fell below 2 for all three complexes, indicating reduced discrimination between cancerous and healthy cells. While octyl-biguanide displayed the highest initial selectivity, this advantage was largely lost in **IRB1**. Similarly, both phenformin and PEB-biguanide showed diminished selectivity upon complexation in **IRB2** and **IRB3**, respectively. These findings underscore the potential of iridium coordination to enhance cytotoxic efficacy, but also highlight the need for further structural optimization to restore or improve selectivity and minimize off-target effects in healthy tissues.

To decipher the mechanism of action of these efficient biguanide–iridium(III) complexes, we decided to leverage the intrinsic fluorescence properties of the complexes. Indeed, iridium complexes are known to have intrinsic fluorescence properties, that can be used to image their cellular uptake and their potential biological targets. We recorded the excitation and emission spectra of biguanide–iridium(III) complexes **IRB1–IRB3** and saw that they emit a strong fluorescence between 450 nm and 600 nm (Table 2) with PLQYs of 0.4–0.58.

To elucidate the intracellular localization of our biguanide–iridium(III) complexes, we employed fluorescence microscopy.

Table 2 Excitation and emission maxima and average photoluminescence quantum yields of **IRB1–IRB3**. Samples were dissolved in chloroform, degassed with Argon, and spectra were recorded at 298 K[a]

Ir(III) complex	Excitation maxima (nm)	Emission maxima (nm)	PLQY (%)
IRB1	278	501	40
IRB2	280	501	45
IRB3	286	501	58

[a] Details on sample preparation and measurements are available in the SI.

Given the well-documented mitochondrial affinity of both biguanides and iridium(III) complexes, we hypothesized mitochondrial targeting by our compounds. To validate this, pancreatic cancer KP4 cells were co-stained with Mitotracker® Deep Red (MTDR) and treated with complexes **IRB1–IRB3** for 24 hours (Fig. 2A). The pronounced colocalization observed between the complexes and MTDR confirmed their mitochondrial accumulation.

To further investigate the kinetics of mitochondrial targeting, we conducted time-course studies at 4 hours, 2 hours, and 30 minutes post-treatment (Fig. 2B–D). Remarkably, all three complexes exhibited rapid mitochondrial localization within 30 minutes of exposure. This swift targeting likely underpins the low nanomolar IC_{50} values observed, as even minimal concentrations rapidly reach mitochondria to initiate antiproliferative effects. Additionally, the sustained presence of **IRB1–IRB3** within mitochondria after 24 hours suggests prolonged mitochondrial engagement, which likely contributes to durable antiproliferative activity.

To delineate the mechanism underlying the antiproliferative effects of our biguanide–iridium(III) complexes, we next investigated their impact on mitochondrial respiratory chain function. Mitochondria-targeting agents frequently disrupt specific respiratory complexes, impairing oxidative phosphorylation (OXPHOS). To probe this, we conducted combination treatments of **IRB1–IRB3** with 2-deoxyglucose (2-DG), a glycolytic inhibitor that impedes the compensatory glycolytic pathway often upregulated in cancer cells harbouring mitochondrial dysfunction.

KP4 pancreatic cancer cells were exposed to sub-IC_{50} concentrations ($0.5 \times IC_{50}$) of **IRB1–IRB3** alone or in combination with 1 mM 2-DG, and cell proliferation was assessed (Fig. 3). In the event of respiratory chain inhibition by the complexes, dual blockade of OXPHOS and glycolysis would be expected to synergistically reduce cellular growth compared to treatment with complexes alone. Consistent with this hypothesis, all combined treatments exhibited significantly diminished relative cell growth relative to monotherapy, confirming that our biguanide–iridium(III) complexes impair mitochondrial respiration.

Notably, **IRB3**, bearing the PEB-biguanide ligand, demonstrated the most pronounced enhancement of growth inhibition in combination with 2-DG, aligning with previous findings that PEB-biguanide derivatives mediate antiproliferative activity through mitochondrial respiratory inhibition. These data collectively substantiate that **IRB3**'s mechanism involves targeted disruption of mitochondrial bioenergetics, potentiated by concomitant glycolytic suppression.

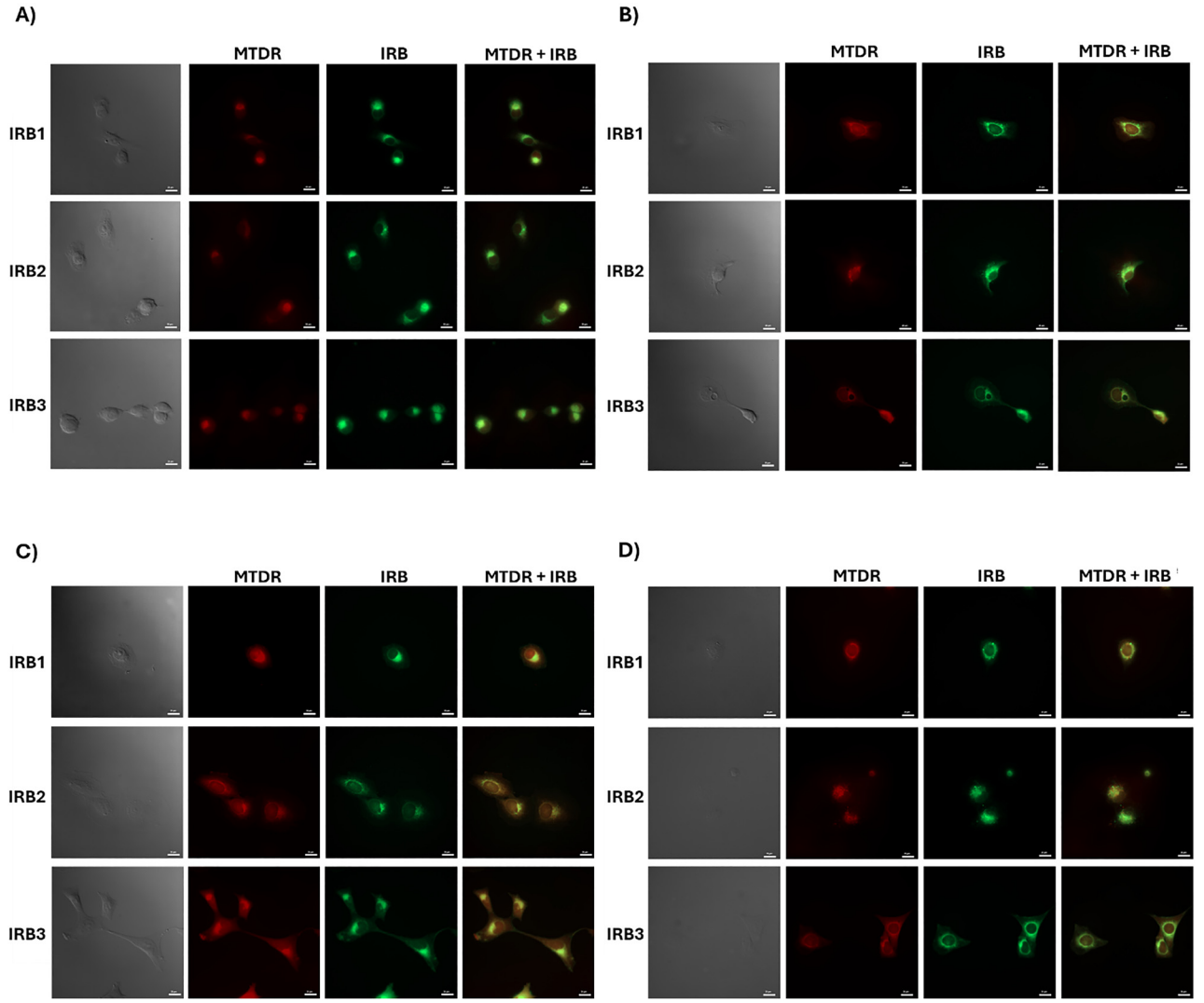

Fig. 2 Confocal microscopy images of KP4 pancreatic cancer cells treated with 100 nM of biguanide–iridium(III) complexes and colocalization with MitoTracker Deep Red (objective 63×, scale bar 20 μm). (A) 24 h treatment (**IRB1** r_P = 0.94; **IRB2** r_P = 0.90; **IRB3** r_P = 0.95). (B) 4 h treatment (**IRB1** r_P = 0.91; **IRB2** r_P = 0.90; **IRB3** r_P = 0.94). (C) 2 h treatment (**IRB1** r_P = 0.90; **IRB2** r_P = 0.92; **IRB3** r_P = 0.94). (D) 30 min treatment (**IRB1** r_P = 0.90; **IRB2** r_P = 0.85; **IRB3** r_P = 0.96). DMSO-treated cells served as negative control, and measurements were performed in triplicate.

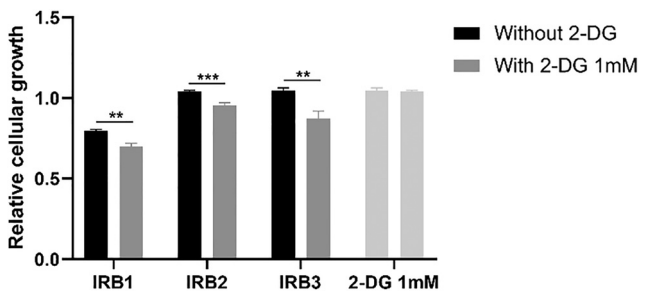

Fig. 3 Relative cellular growth of KP4 cells treated with sub-IC_{50} concentrations (0.5 × IC_{50}) of **IRB1–IRB3** (0.6 μM of **IRB1**, 1.2 μM of **IRB2** and 0.6 μM of **IRB3**), with and without 1 mM 2-DG (** = $p < 0.01$, *** = $p < 0.001$). Measurements were performed in triplicate.

In summary, we developed three novel biguanide–iridium(III) complexes exhibiting potent antiproliferative activity against pancreatic cancer cells, surpassing that of their free biguanide ligands. While increased toxicity toward healthy cells underscores the need for improved cancer selectivity, their intrinsic fluorescence enabled rapid mitochondrial localization within 30 minutes, sustained up to 24 hours. Preliminary studies suggest disruption of the mitochondrial respiratory chain as a key mechanism of action. These findings establish biguanide–iridium conjugation as a promising strategy for mitochondria-targeted anticancer therapeutics and their use in photodynamic therapy should be studied in the future.

Author contributions

A. R. S. and B. A. B. for conceptualization of the project. S. L., E. S. and P. M. for investigation and synthesis of the compounds

and biological studies. R. S. H. for ligand-exchange studies and compounds purity. S. L. for the original draft preparation. A. R. S. and B. A. B. for writing, review and editing. All authors have given approval to the final version of the manuscript.

Conflicts of interest

There are no conflicts to declare.

Data availability

The data supporting this article have been included as part of the supplementary information (SI). Supplementary information: synthetic procedures, fluorescence studies and biological assays. See DOI: https://doi.org/10.1039/d5nj04288g.

Notes and references

1 J. S. Armstrong, *Br. J. Pharmacol.*, 2007, **151**(8), 1154–1165.
2 H. Wang, B. Fang, B. Peng, L. Wang, Y. Xue, H. Bai, S. Lu, N. H. Voelcker, L. Li, L. Fu and W. Huang, *Front. Chem.*, 2021, **9**, 683220.
3 F. Fontanesi, Mitochondria: Structure and Role in Respiration, In eLS, pp. 1–13.
4 C. Wang and R. J. Youle, *Annu. Rev. Genet.*, 2009, **43**, 95–118.
5 F. J. Bock and S. W. G. Tait, *Nat. Rev. Mol. Cell Biol.*, 2020, **21**(2), 85–100.
6 T. T. Nguyen, S. Wei, T. H. Nguyen, Y. Jo, Y. Zhang, W. Park, K. Gariani, C.-M. Oh, H. H. Kim, K.-T. Ha, K. S. Park, R. Park, I.-K. Lee, M. Shong, R. H. Houtkooper and D. Ryu, *Exp. Mol. Med.*, 2023, **55**(8), 1595–1619.
7 D. R. Green and J. C. Reed, *Science*, 1998, **281**(5381), 1309–1312.
8 L. D. Zorova, V. A. Popkov, E. Y. Plotnikov, D. N. Silachev, I. B. Pevzner, S. S. Jankauskas, V. A. Babenko, S. D. Zorov, A. V. Balakireva, M. Juhaszova, S. J. Sollott and D. B. Zorov, *Anal. Biochem.*, 2018, **552**, 50–59.
9 J. D. Ly, D. R. Grubb and A. Lawen, *Apoptosis*, 2003, **8**(2), 115–128.
10 G. Eibl and E. Rozengurt, *Cancer Metastasis Rev.*, 2021, **40**(3), 865–878.
11 E. H. Kim, J. H. Lee, Y. Oh, I. Koh, J. K. Shim, J. Park, J. Choi, M. Yun, J. Y. Jeon, Y. M. Huh, J. H. Chang, S. H. Kim, K. S. Kim, J. H. Cheong, P. Kim and S. G. Kang, *Neuro-Oncol.*, 2017, **19**(2), 197–207.
12 N. Saini and X. Yang, *Acta Biochim. Biophys. Sin.*, 2018, **50**(2), 133–143.
13 S. Andrzejewski, S.-P. Gravel, M. Pollak and J. St-Pierre, *Cancer Metabolism*, 2014, **2**(1), 12.
14 H. R. Bridges, J. N. Blaza, Z. Yin, I. Chung, M. N. Pollak and J. Hirst, *Science*, 2023, **379**(6630), 351–357.
15 H. R. Bridges, A. J. Jones, M. N. Pollak and J. Hirst, *Biochem. J.*, 2014, **462**(3), 475–487.
16 H. R. Bridges, V. A. Sirviö, A.-N. A. Agip and J. Hirst, *BMC Biol.*, 2016, **14**(1), 65.
17 A. R. Cameron, L. Logie, K. Patel, S. Erhardt, S. Bacon, P. Middleton, J. Harthill, C. Forteath, J. T. Coats, C. Kerr, H. Curry, D. Stewart, K. Sakamoto, P. Repiščák, M. J. Paterson, I. Hassinen, G. McDougall and G. Rena, *Redox Biol.*, 2018, **14**, 187–197.
18 B. Kalyanaraman, G. Cheng, M. Hardy, O. Ouari, M. Lopez, J. Joseph, J. Zielonka and M. B. Dwinell, *Redox Biol.*, 2018, **14**, 316–327.
19 M. R. Owen, E. Doran and A. P. Halestrap, *Biochem. J.*, 2000, **348**(Pt 3), 607–614.
20 M. Parisotto, N. Vuong-Robillard, P. Kalegari, T. Meharwade, L. Joumier, S. Igelmann, V. Bourdeau, M. C. Rowell, M. Pollak, M. Malleshaiah, A. Schmitzer and G. Ferbeyre, *Cancers*, 2022, **14**(22), 5597.
21 A. Pecinova, Z. Drahota, J. Kovalcikova, N. Kovarova, P. Pecina, L. Alan, M. Zima, J. Houstek and T. Mracek, *Oxid. Med. Cell. Longevity*, 2017, **2017**, 7038603.
22 S. C. Navdeep, D. Avizonis, R. R. Colleen, E. W. Samuel, S. Menz, R. Neuhaus, S. Christian, A. Haegebarth, C. Algire and M. Pollak, *Cell Metab.*, 2016, **23**(4), 569–570.
23 G. S. Wang and C. Hoyte, *J. Intensive Care Med.*, 2019, **34**(11–12), 863–876.
24 A. Hébert, M. Parisotto, G. Ferbeyre and A. R. Schmitzer, *Supramol. Chem.*, 2019, **31**(3), 127–139.
25 (*a*) A. Hébert, M. Parisotto, M.-C. Rowell, A. Doré, A. Fernandez Ruiz, G. Lefrançois, P. Kalegari, G. Ferbeyre and A. R. Schmitzer, *Sci. Rep.*, 2021, **11**(1), 9854; (*b*) M. Petit, E. Dubas Prade and A. R. Schmitzer, *ACS Bio. Med. Chem. Au*, 2025, **5**(4), 553–564.
26 (*a*) L. Wang, R. Guan, L. Xie, X. Liao, K. Xiong, T. W. Rees, Y. Chen, L. Ji and H. Chao, *Angew. Chem., Int. Ed.*, 2021, **60**(9), 4657–4665; (*b*) J. S. Nam, M. G. Kang, J. Kang, S. Y. Park, S. J. C. Lee, H. T. Kim, J. K. Seo, O. H. Kwon, M. H. Lim, H. W. Rhee and T. H. Kwon, *J. Am. Chem. Soc.*, 2016, **138**(34), 10968; (*c*) F. X. Wang, M. H. Chen and X. Y. Hu, *Sci. Rep.*, 2016, **6**, 38954.
27 Y. Su, J. Yang, M.-M. Wang, H.-B. Fang, H.-K. Liu, Z.-H. Yu and Z. Su, *J. Inorg. Biochem.*, 2024, **251**, 112427.
28 D. L. Ma, C. Wu, K. J. Wu and C. H. Leung, *Molecules*, 2019, **24**(15), 2739.
29 Y. Wu, J. Liu, M. Shao, P. Zhang, S. Song, G. Yang, X. Liu and Z. Liu, *J. Inorg. Biochem.*, 2022, **233**, 111855.
30 T. Yang, M. Zhu, M. Jiang, F. Yang and Z. Zhang, *Front. Pharmacol.*, 2022, **13**, 1025544.
31 J. Yang, H.-J. Fang, Q. Cao and Z.-W. Mao, *Chem. Commun.*, 2021, **57**(9), 1093–1096.

